CARBON letters

Note

Carbon Letters Vol. 26, 102-106 (2018)

Fabrication of electrochemical double-layer capacitor electrode using an activated carbon fiber network

Wan Jin Kim[1], Jun Young Yoon[2], Tae Hoon Ko[1], Byoung-Suhk Kim[1,3,♠], and Yong Sik Chung[1,♠]

[1]Department of Organic Materials & Fiber Engineering, Chonbuk National University, 567 Baekje-daero, Deokjin-gu, Jeonju-si, Jeollabuk-do 54896, Republic of Korea

[2]Kolon Industries, Inc., KOLON Tower, Gwacheon 13837, Korea

[3]Department of BIN Convergence Technology, Chonbuk National University, 567 Baekje-daero, Deokjin-gu, Jeonju-si, Jeollabuk-do 54896, Republic of Korea

Article Info

Received 30 November 2016
Accepted 8 November 2017

♠Corresponding Author
E-mail: psdcolor@jbnu.ac.kr
kbsuhk@jbnu.ac.kr
Tel: +82-63-270-2350
+82-63-270-2352

DOI: http://dx.doi.org/10.5714/CL.2018.26.102

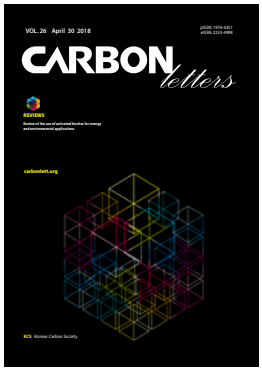

http://carbonlett.org

pISSN: 1976-4251
eISSN: 2233-4998

Due to environmental issues attributed to the use of fossil fuels, considerable interest has recently been shown in fuel cell vehicles, electric vehicles, and hybrid electric vehicles with a combined internal combustion engine and secondary battery. In the case of electric vehicles that momentarily require considerable power, their performance can be significantly improved through the development of an electrochemical double-layer capacitor (EDLC) with high energy efficiency [1-3].

Currently, activated carbons (ACs) and activated carbon fibers (ACFs) possessing high specific accumulation capacity are mainly used as electrode materials for EDLCs due to their excellent properties, such as high specific surface area (SSA), relatively high electronic conductivity, good corrosion resistance, and low thermal expansivity [4,5]. ACFs are a novel and fibrous adsorbent that have been developed by the carbonization and activation of organic fibers. Their unique properties are attracting attention in fundamental research and in the development of applications [6]. The advantages of ACFs are their smaller fiber diameter (which minimizes diffusion limitations and allows rapid adsorption/desorption), more concentrated pore-size distribution (PSD), and excellent adsorption capacity at low concentration of adsorbates in comparison with conventional activated granular/powder carbons. The porosity of ACFs is developed during activation, normally by partial gasification in steam and/or carbon dioxide, and is influenced by many factors, such as the degree of activation and the conditions used for carbonization. Typically, ACFs are a type of micro-pore carbonous adsorbent exhibiting slit-shaped pores. The properties of porosity, surface area, and surface structure contribute to the high adsorption capacity of ACFs, enabling them to play an important role as an electrode material for EDLCs [7-9].

Generally, the carbon materials used for EDLC electrodes are treated with physical or chemical activations to achieve a surface structure with high porosity and SSA. The activation processes can be divided into physical activation and chemical activation [10-12]. Physical or thermal activation occurs through the introduction of oxidizing gases, normally carbon dioxide, steam, or a mixture of the two [11-13], while chemical activation normally involves chemical activation agents that are usually hydroxides, such as sodium hydroxide (NaOH) and potassium hydroxide (KOH) [14,15], or acids, such as phosphoric acid (H_3PO_4), nitric acid (HNO_3) and sulfuric acid (H_2SO_4) [14].

EDLC electrodes are primarily based on carbon materials [16, 17]. Carbon materials have a variety of geometric shapes when viewed macroscopically, such as zero-dimensional (0D) fullerene or carbon particles, one-dimensional (1D) carbon nanotubes (CNTs) or carbon fibers (CFs), and two-dimensional (2D) graphene, graphite sheets, and so forth. [18]. Among these geometric shapes, 1D and 2D carbon materials have been widely used in binder free electrodes because they can readily form highly conductive and flexible carbon networks (such as fabric, film, paper, and textiles) with outstanding electrochemical performances. These carbon networks are achieved by initially using carbon materials via a variety of methods. El-Kady and others [19] reported that a flexible graphene-based electrode (graphene

films) can be produced by the low-power infrared laser reduction of graphite oxide films with a standard Light Scribe DVD optical drive. Pasta *et al*. [20] fabricated a single-walled carbon-nanotube (SWCNT) textile with a sheet resistance as low as 1 Ω/sq and demonstrated that aqueous supercapacitors made from these textiles in a Li_2SO_4 electrolyte display a specific capacitance of 70-80 F/g at a current density of 0.1 A/g, which rarely decreased after 35,000 cycles. Hu and Cui [21] concluded that coating pseudocapacitor materials (such as MnO_2) onto carbon textiles can greatly increase their specific capacitance. Horng *et al*. [22] fabricated flexible supercapacitors with PANI nanowires/carbon cloth electrodes, resulting in a high capacitance (1079 F/g and 1.8 F/cm^2 for mass and area-normalized capacitance) and a high energy density (100.9 Wh/kg at a power density of 12.1 kW/kg). Wu *et al*. [23] reported that graphene/PANI nanofiber paper was produced by direct filtration of a dispersion consisting of graphene and PANI.

Thus, several efforts have been devoted to the development of carbon network electrodes; however, research has not been performed to develop an ACF network electrode fabricated by the facile network making process. We fabricated an ACF network electrode for EDLCs through a facile network-making process. Analyses of the surface structure and electrochemical performance of the EDLCs were performed to evaluate their potential for application as electrodes.

In this study, ACFs (from An Shan Sino Carbon, China) with a Brunauer-Emmett-Teller (BET) surface area of 1,200 m^2/g and a fiber length of 6 mm were used to fabricate an ACF network, whereby extra purification or treatment was not performed for the ACFs. For the dimensional stability of the ACF network, the physical bonding between ACFs in the network was induced by introducing aqueous phenol resin (Phenolite KC-6301, Kangnam Chemical Co. Ltd., Korea) as a binding material.

To prepare a uniformly dispersed ACF slurry, ACFs were added to a 10 wt.% phenol aqueous solution and then stirred using a mechanical stirrer for 10 min. The ACF network was fabricated by the filtering and dehydration of the resulting slurry on a screen mesh embedded in the network-making process. A circular ACF network with a diameter of 160 mm was obtained through these procedures. The ACF network was dried at 80°C for 60 min, and was then further pressed using a hot-pressing machine at 130 °C for 5 min. To improve the dimensional stability of the ACF network during the activation process, the network was carbonized using a horizontal tubular furnace (Pyrotech Co. Ltd., Korea) at 900°C for 30 min under an N_2 atmosphere [24].

The thermal decomposition characteristics of the ACF network were analyzed to determine the optimal activation temperature range using a thermogravimetric analyzer (TGA, Rigaku, Japan). TGA thermograms were investigated from room temperature to 700°C with heating rate of 10°C/min. To activate the network under O_2 oxidizing gas, a horizontal tubular furnace was heated with a heating rate of 10°C/min, and the ACF network was then activated for 30 min at 300°C. The morphology of the ACF network were then observed by field-emission scanning electron microscopy (FE-SEM).

The electrochemical performance was determined in the electrochemical cell with a three-electrode system using cyclic voltammetry (Metrohm Autolab, AUT302M, FRA2). An H_2SO_4 aqueous solution was employed as an electrolyte. Platinum wire and Ag/AgCl were used as the counter electrode and reference electrode, respectively. The ACF network was utilized as the working electrode in this study, and it was applied directly without the addition of any binder or conductive materials.

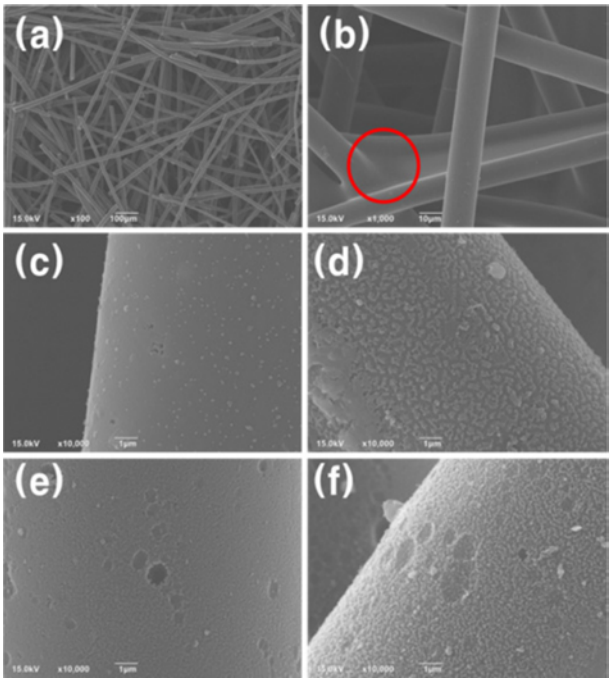

Fig. 1. SEM images of ACF network (a), (b), ACF surface activated at 300 °C (c), 325 °C (d), 350 °C (e), and 375 °C (f) for 30 min under O_2 oxidizing gas.

Fig. 1 shows SEM images of the ACF network carbonized at 900°C for 30 min under an N_2 atmosphere. The images show that the ACFs have a smooth surface morphology and are randomly distributed in the network (Fig. 1(a)). As indicated by the circle in Fig. 1(b), many ACFs are physically connected by phenol resin, which provides the dimension stability of the ACF network. Also, the physical connection between the ACFs may lead to higher electrical conductivity of the ACF network electrode.

Conventionally, carbon materials are chemically treated with a strong alkaline solution or thermally treated above 800 °C under oxidizing gases to improve the porous surface structure. However, these chemical treatments cause severe defects in the carbon materials, resulting in lower crystallinity and a poor carbon yield [25]. In this study, the physical activation was conducted at a relatively low temperature in O_2 oxidizing gas to improve the electrochemical performance of the ACF network electrodes. Prior to the activation, TGA thermograms of the ACF network were taken to determine the optimal activation temperature range. As shown in Fig. 2, weight loss of the ACF network started at 300 °C, and a weight loss of about 98% was then reached at 500 °C.

Based on these TGA results, ACF networks were activated at 300, 325, 350, and 375 °C (heating rate of 10 °C/min) for 30 min under O_2 oxidizing gas. Figures 1(c) to 1(f) exhibit SEM images of the ACF networks activated at different temperatures. Numerous pores developed in the ACF surface due to the gas-

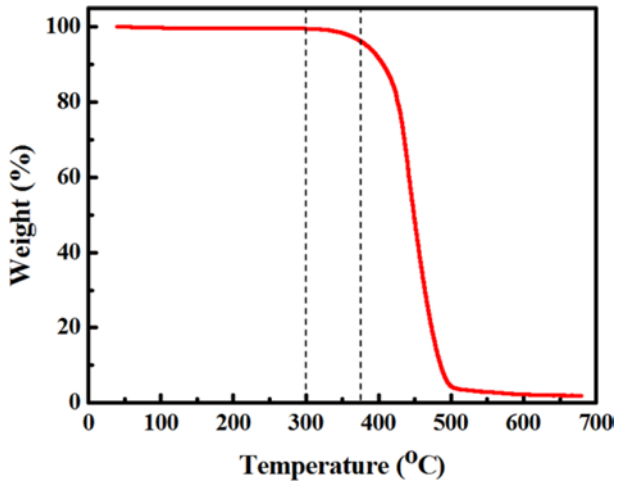

Fig. 2. Thermogravimetric analysis of the ACF network at a heating rate of 10 °C/min under an air atmosphere [27].

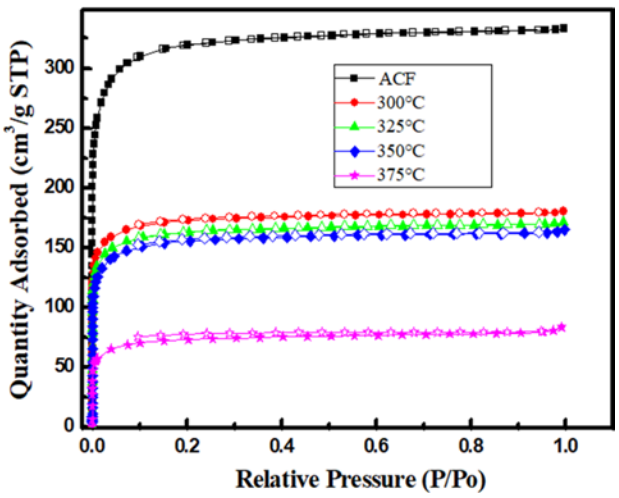

Fig. 3. N_2 adsorption/desorption isotherms of ACF network electrodes activated at various temperatures [27].

ification of carbon atoms by O_2 oxidizing gas during activation. This suggests that a higher activation temperature is more efficient for pore formation. However, the dimensional stabilities of the ACF networks activated at 300 °C and 325 °C were well maintained, while those of the ACF networks activated at 350 °C and 375 °C had collapsed. Therefore, ACF networks activated at 350 °C and 375 °C cannot be used as network electrodes due to their collapsed form, despite their excellent porosity and surface structure.

Table 1 lists the specific surface areas and pore structures of the ACF network electrodes activated at various temperatures. It shows that all the samples have a large micro-pore volume with a diameter of approximately 2 nm. As the activation temperature increases, meso-pores with a size of 2 nm or larger begin to develop, and the average pore diameter expands. In contrast, the specific surface area and the total pore volume decrease with increasing activation temperature. Fig. 3 shows the isotherms of all the samples appearing to be Type I according to the IUPAC classification, implying that they mostly include micro-pores. The absence of a hysteresis loop between the adsorption and desorption isotherms means that the pores are tubular or wedge-shaped. Meanwhile, the ACF network electrodes activated at 375 °C exhibited a hysteresis loop due to the capillary condensation of nitrogen in the increased meso-pores formed at a higher activation temperature.

Cyclic voltammetry (CV) studies were performed to analyze the capacitance behavior of the ACF network electrodes at a scan rate of 50 mV/s in 0.5 M H_2SO_4 aqueous solution. As seen in Fig. 4(a), the CV curves have an almost rectangular shape, indicating the ideal capacitive behavior of the ACF networks [26]. Moreover, the capacitance behavior of the ACF network electrodes was enhanced with increasing activation temperature up to 350 °C. However, the specific capacitance of the ACF network electrode activated at 375 °C was decreased. It is believed that the number of micro-pores of the electrode was reduced because of the excessively high activation temperature, which caused the collapse or enlargement of the pore walls. Also, it can be seen that the ACF network electrodes have redox peaks at a potential of approximately 0.4 V. This suggests that oxidation-reduction reaction occurred due to the oxygen functional groups introduced during O_2 activation. Fig. 4(b) shows the electrochemical impedance spectroscopy (EIS) behavior of the ACF network electrodes activated at various temperatures. In the high-frequency range, the shape of the ACF network electrodes is a small semicircle, which corresponds to the charge transfer resistance (RCT, Ω) resulting from electron diffusion. The result demonstrates that ACF network electrodes can provide a conve-

Table 1. Specific surface area and pore structures of ACF network electrodes activated at various temperatures [27].

	SSA (m^2/g)	V_{total} (cm^3/g)	V_{micro} (%)	$V_{meso\&macro}$ (%)	D_{ave} (nm)
ACF	1256	0.515	91.5	8.5	1.637
300 °C	674	0.278	92.1	7.9	1.651
325 °C	634	0.264	91.3	8.7	1.666
350 °C	606	0.254	89.8	10.2	1.675
375 °C	281	0.129	81.4	18.6	1.829

SSA: specific surface area, V_{total}: total pore volume, V_{micro}: micro-pore volume, $V_{meso\&macro}$: meso & macro-pore volume, D_{ave}: average pore diameter.

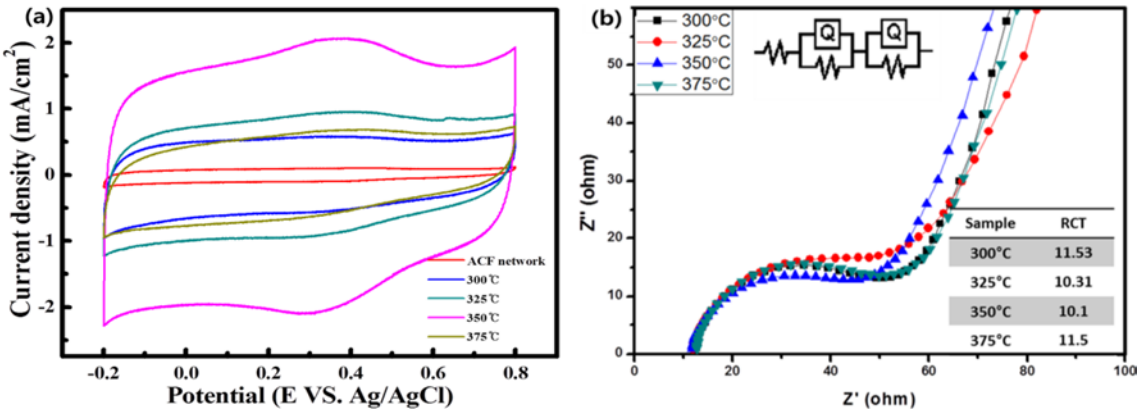

Fig. 4. Cyclic voltammograms (a) and electrochemical impedance spectroscopy (EIS) curves (b) of ACF network electrodes activated at various temperatures.

nient pathway for ion and electron transport.

In summary, we fabricated ACF networks using a facile network-making method for application as electrodes for EDLCs. Commercial ACFs were used for network fabrication, and phenol resin was employed as a binding material for the dimensional stability of the ACF networks. Also, O_2 activation was conducted to improve the electrochemical performance. The fabricated ACF network electrodes were used as working electrodes. From the CV results, the ACF network electrodes exhibited ideal capacitive behavior with an almost rectangular shape, and redox peaks due to the Faradaic reaction were observed because of the functional groups generated by O_2 activation.

Acknowledgment

This paper was supported by research funds of Chonbuk National University in 2011.

References

[1] Y. Nagao, Y. Nakayama, H. Oda, and M. Ishikawa, Activation of an ionic liquid electrolyte for electric double layer capacitors by addition of BaTiO3 to carbon electrodes, Journal of Power Sources 166, 595-598 (2007).

[2] Q.Y. Lia, Z.S. Lia, L. Lina, X.Y. Wang, Y.F. Wang, C.H. Zhanga, H.Q. Wang, Facile synthesis of activated carbon/carbon nanotubes compound for supercapacitor application, Chemical Engineering Journal 156, 500-504 (2010).

[3] D.W. Jung, C.S. Lee, S. Park, E.S. Oh, Characterization of electric double-layer capacitors with carbon nanotubes directly synthesized on a copper plate as a current collector, Kor. J. Met. Mater. 49, 419-424 (2010).

[4] X. Li, C. Han, X. Chen, C. Shi, Preparation and performance of straw based activated carbon for supercapacitor in non-aqueous electrolytes, Microporous and Mesoporous Materials 131, 303-309 (2010).

[5] H. Wang, Y. Zhong, Q. Li, J. Yang, Q. Dai, Cationic starch as a precursor to prepare porous activated carbon for application in supercapacitor electrodes, Journal of Physics and Chemistry of Solids 69 2420-2425 (2008).

[6] M. Suzuki, Activated carbon fiber: Fundamentals and applications, Carbon 32, 577-586 (1994).

[7] Z. Ryu, J. Zheng, M. Wang, Porous Structure of PAN-based activated carbon fibers, Carbon 36, 427-432 (1998).

[8] M. Enterria, F.J. Martin-Jimeno, F. Suarez-Garcia, J.I. Paredes, M.F.R. Pereira, J.I. Martins, A. Martinez-Alonso, J.M.D. Tascon, J.L. Figueiredo, Effect of nanostructure on the supercapacitor performance of activated carbon xerogels obtained from hydrothermally carbonized glucose-graphene oxide hybrids, Carbon, 105, 474-483 (2016).

[9] J. Pu, C. Li, L. Tang, T. Li, L. Ling, K. Zhang, Y. Xu, Q. Li, Y. Yao, Impregnation assisted synthesis of 3D nitrogen-doped porous carbon with high capacitance, Carbon 94, 650-660 (2015).

[10] J. Yan, T. Wei, B. Shao, F. Ma, Z. Fan, M. Zhang, C. Zheng, Y. Shang, W. Qian, F. Wei, Electrochemical properties of graphene nanosheet/carbon black composites as electrodes for supercapacitors, Carbon 48, 1731-1737 (2010).

[11] T. Burchell, Carbon fiber composite adsorbent media for low pressure natural gas storage, Energia 13, 1-5 (2002).

[12] J.A. Maciá-Agulló, B.C. Moore, D. Cazorla-Amorós, A. Linares-Solano, Influence of carbon fibres crystallinities on their chemical activation by KOH and NaOH, Microporous and Mesoporous Materials 101, 397-405 (2007).

[13] T.H. Ko, P. chiranairadul, C.K. Lu, C.H. Lin, The effects of activation by carbon dioxide on the mechanical properties and structure of PAN-based activated carbon fibers, Carbon 30, 647-655 (1992).

[14] A.H. Lu, J.T. Zheng, Study of microstructure of high-surface-area polyacrylonitrile activated carbon fibers, Journal of Colloid and Interface Science 236, 369-374 (2001).

[15] Z. Ryu, H. Rong, J. Zheng, M. Wang, B Zhang, Microstructure and chemical analysis of PAN-based activated carbon fibers prepared by different activation methods, Carbon, 40, 1144-1147 (2002).

[16] V.L. Pushparaj, M.M. Shaijumon, A. Kumar, S. Murugesan, L. Ci, R. Vajtai, Flexible energy storage devices based on nanocomposite paper, Proceedings of the National Academy of Sciences of the United States of America, 104, 13574-13577 (2007).

[17] D.W. Wang, F. Li, J. Zhao, W. Ren, Z.G. Chen, J. Tan, Fabrication of graphene/polyaniline composite paper via in situ anodic elec-

tropolymerization for high-performance flexible electrode, ACS Nano, 3, 1745-1752 (2009).
[18] S. Shi, C. Xu, C. Yang, J. Li, H. Du, B. Li, F. Kang, Flexible supercapacitors, Particuology, 11, 371-377 (2013).
[19] M. F. El-Kady, V. Strong, S. Dubin, R.B. Kaner, Laser scribing of high-performance and flexible graphene-based electrochemical capacitors, Science, 335, 1326-1330 (2012).
[20] M. Pasta, F.L. Mantia, L. Hu, H.D. Deshazer, Y. Cui, Aqueous supercapacitors on conductive cotton, Nano Research, 3, 452-458 (2010).
[21] L. Hu, Y. Cui, Energy and environmental nanotechnology in conductive paper and textiles, Energy & Environmental Science, 5, 6423-6435 (2012).
[22] Y.Y. Horng, Y.C. Lu, Y.K. Hsu, C.C. Chen, L.C. Chen, K.H. Chen, Flexible supercapacitor based on polyaniline nanowires/carbon cloth with both high gravimetric and area-normalized capacitance, Journal of Power Sources, 195, 4418-4422 (2010).
[23] Q. Wu, Y. Xu, Z. Yao, A. Liu, G. Shi, Supercapacitors based on flexible graphene/polyaniline nanofiber composite films, ACS Nano, 4, 1963-1970 (2010).
[24] J.C. Lee, B.H. Lee, B.G. Kim, M.J. Park, D.Y. Lee, I.H. Kuk, H. Chung, H.S. Kang, H.S. Lee, D.H. Ahn, The effect of carbonization temperature of PAN fiber on the properties of activated carbon fiber composites, Carbon, 35, 1479-1484 (1997).
[25] H.I. Joh, H.K. Song, K.B. Yi, S. Lee, The production of porosity in carbon nanofibers by the catalytic action of Ni nanoparticles in low temperature activation, Carbon 53, 399-413 (2013).
[26] E. Frackowiak, F. Beguin, Carbon materials for the electrochemical storage of energy in capacitors, Carbon 39, 937-950 (2001).
[27] W. J. Kim, T. H. Ko, M. K. Seo, Y. S. Chung, H. Y. Kim, B. S. Kim, Engineered carbon fiber papers as flexible binder-free electrodes for high-performance capactive energy storage, Journal of Industrial and Engineering Chemistry 59, 277-285 (2018).